Atmos. Chem. Phys. Discuss., 4, 5655–5681, 2004
www.atmos-chem-phys.org/acpd/4/5655/
SRef-ID: 1680-7375/acpd/2004-4-5655

Atmospheric Chemistry and Physics Discussions

High resolution mid-infrared cross-sections for peroxyacetyl nitrate (PAN) vapour

G. Allen[1], **J. J. Remedios**[1], **D. A. Newnham**[2,*], **K. M. Smith**[2], **and P. S. Monks**[3]

[1]EOS, Space Research Centre, Dept. of Physics and Astronomy, Univ. Leicester, Leicester, LE1 7RH, UK
[2]Space Science & Technology Dept., Rutherford Appleton Lab., Didcot, Oxon, OX11 0QX, UK
[3]Department of Chemistry, Univ. Leicester, Leicester, LE1 7RH, UK
[*]now at: TeraView Limited, 302/304 Science Park, Milton Road, Cambridge, CB4 0WG, UK

Received: 8 July 2004 – Accepted: 1 September 2004 – Published: 22 September 2004

Correspondence to: G. Allen (ga15@le.ac.uk)

Abstract

Absorption spectra of peroxyacetyl nitrate (PAN, $CH_3C(O)OONO_2$) vapour at room temperature (295 K) have been measured in the mid-infrared range, 550–2200 cm^{-1} (18.2–3.33 μm), using a Fourier transform infrared spectrometer at instrument resolutions of 0.25 and 0.03 cm^{-1} (unapodised). Both cross-section data and integrated absorption intensities for the five principal bands in the PAN spectra in this spectral range have been derived from fourteen separate PAN transmission spectra measurements. Band intensities and band centre absorptivities are also reported for four weaker PAN absorption bands in the mid infrared for the first time. These observations are the highest spectral resolution measurements of PAN bands recorded in the infrared to date. For three of the five strongest bands, the absolute integrated absorption intensities are in excellent agreement with previous studies. A 4.8% lower integrated intensity was found for the 1741 cm^{-1} ν_{as} (NO_2) PAN absorption band, possibly as a result of the removal in this work of spectra affected by subtle acetone contamination, while a 10.6% higher intensity was determined for the 1163 cm^{-1} ν (C-O) absorption band. No direct effects of spectral resolution were observed. The improved accuracy of these absorption cross-sections will allow more accurate investigations of PAN using infrared spectroscopy, particularly for remote sensing of PAN in the atmosphere.

1. Introduction

Peroxyacetyl nitrate (PAN) is an important atmospheric trace species through its role as a reservoir of the active nitrogen compound, NO_2, and through its impact on the oxidising potential of the atmosphere. The PAN compound is formed in the atmosphere by the oxidation of acetaldehyde and further reaction with nitrogen dioxide (Singh, 1987). In the atmosphere, the highest concentrations of PAN are often found in so-called photochemical smog episodes, such as Los Angeles smog events where it was first noted by Stephens (1964). The chief loss mechanism for PAN in the lower troposphere is

ACPD

4, 5655–5681, 2004

thermolysis, which occurs readily at temperatures above 273 K with a PAN lifetime of a matter of hours (Kirchener et al., 1999). However, this thermolysis rate drops quickly with temperature allowing lifetimes in the order of months against thermolysis in the cold upper troposphere (of order 200K). In this region of the atmosphere, the photolysis rate becomes dominant and hence the species can be an important indicator of the photochemical age of polluted airmasses. The long lifetime of PAN in the upper troposphere allows it to transport NO_2 over wide areas, taking NO_2 from polluted regions and releasing it in remote pristine locations where active nitrogen chemistry can influence the production of surface ozone (Olszyna et al., 1994).

It has now become clear that PAN is one of the most important reservoirs of active nitrogen in the troposphere and, in some regions, is the dominant form of odd nitrogen, NO_y (where NO_y=NO+NO_2+reservoir compounds). PAN also has an effect on the oxidising power of the atmosphere through its reaction with the hydroxyl radical, OH (Talukdar et al., 1995).

In the atmosphere, PAN has only been measured by in situ studies such as those made by Gas Chromatography Electron Capture Detection (GC-ECD) techniques (Tanimoto et al., 1999) during aircraft campaigns such as those detailed by Emmons et al. (1997). The typically low concentrations of PAN (<100 pptv) make it difficult to detect by these methods and errors remain high (typically 30%), with a limit of detection of around 5 pptv. New satellite missions could provide an alternative means to remotely detect trace organic species on a global scale through their characteristic infrared signature. The Michelson Interferometer for Passive Atmospheric Sounding (Nett et al., 2001) onboard the European Space Agency's Envisat platform (Louet, 2001) launched in March 2002, is one such instrument to exploit the potential of using infrared limb emission spectra measured at high spectral resolution to retrieve profile information for trace atmospheric species (Fischer and Oelhaf, 1996).

The retrieval of concentration data from satellite-derived spectra requires accurate reference cross-sections measured in the laboratory at sufficiently high spectral resolution. The high resolution is important for two reasons: 1) accurate calculation of

radiative transfer in the atmosphere requires knowledge of spectroscopic behaviour to within the typical separations of overlapping lines (less than 0.1 cm^{-1} for the troposphere where PAN is important); 2) the MIPAS instrument has an unapodised spectral resolution of 0.025 cm^{-1} and is therefore sensitive to spectral detail at this level. Thus appropriate data for PAN is a prerequisite for studies to examine the spectral signature of this gas in infrared remote sensing data.

In this paper, we report the first data for the infrared absorption cross-sections of PAN vapour to be obtained at spectral resolutions greater than 0.1 cm^{-1}. The new spectral data for PAN will allow greater confidence in identification of PAN effects in infra-red spectra ranging from the MIPAS example discussed here to air quality measurements to laboratory investigations of PAN and related compounds.

2. Experimental details

The spectra presented here were recorded using the Bruker IFS 120HR Fourier transform infrared (FTIR) spectrometer at the Molecular Spectroscopy Facility, Rutherford Appleton Laboratory, UK. The configuration of the instrument for the measurements reported here is listed in Table 1. The apparatus consisted of an evacuated 26.1 cm path length glass absorption cell equipped with potassium bromide windows interfaced to a customised gas handling vacuum line.

Three overlapping spectra regions in the mid-infrared were measured using appropriate optical and electronic filters. The use of optical filters covering a narrow spectral range improves signal to noise and reduces the effects of detector non-linearity. Both DLaTGS and liquid nitrogen cooled MCT detectors were used, giving excellent signal to noise over the region of interest (typically better than 500:1 after co-addition at 1740.5 cm^{-1}). Of the measurements employed in the data analysis, six measurements were obtained at 0.25 cm^{-1} resolution in the range 550–1650 cm^{-1} and four in the 1650–2200 cm^{-1} region with a further four measurements recorded over the wider 600–1900 cm^{-1} area at a higher resolution of 0.03 cm^{-1}.

ACPD
4, 5655–5681, 2004

Pressure was monitored throughout the measurements by calibrated MKS Baratron pressure gauges (10 and 1000 Torr) with an accuracy of $\pm 0.5 \times 10^{-4}$ Torr or 0.3% of measured pressure. To avoid decomposition or detonation of the PAN sample, the Baratron gauges were operated at room temperature rather than at the normal 40°C thermostated operating temperature. At the air-conditioned laboratory temperature of 295 ±1 K, the error in the Baratron calibration due to operation at the lower temperature was determined to be negligible by monitoring the pressure of a stable nitrogen gas sample over a period of two hours whilst monitoring changes in laboratory temperature. The difference between the heated and unheated readings over a period of two hours was indistinguishable from the small leak rate measured for the gas handling line.

The leak rate of air into the absorption cell via the vacuum line was periodically measured and included in the procedure for estimating the partial pressure of PAN employed in calculating the final cross-section. Cell temperature was monitored by a series of eight platinum resistance (PT100) thermometers, with a typical mean accuracy of 0.1 K, attached in thermal contact with the external walls of the absorption cell.

The recorded spectra were averaged from 50 co-added scans at unapodised resolutions of 0.25 and 0.03 cm^{-1} (where resolution is defined here as 0.9/maximum optical path difference). Transmission spectra were calculated by ratioing PAN sample spectra with the average of background spectra recorded immediately before and after each sample measurement. A total of fourteen PAN spectra were successfully recorded over a pressure range of 0.24–2.20 hPa and employed in the data analysis to obtain absorptivities and integrated intensities.

Since PAN is not commercially available, samples were prepared by the nitration of peracetic acid in the following synthesis based on the method detailed by Gaffney et al. (1984) and Nielsen et al. (1982). Peracetic acid (30% w/v) was first prepared by the equilibrium reaction between hydrogen peroxide (30% w/v), sulphuric acid (99.999% w/v) and glacial acetic acid. The peracetic acid mixture was then added slowly to a mixture of dodecane (cooled to 1–3°C), fuming nitric acid and sulphuric acid (99.999%

ACPD
4, 5655–5681, 2004

w/v). The organic product was dried with anhydrous magnesium sulphate and dissolved in dodecane. The success of the synthesis was tested spectroscopically for the first samples using a low-resolution Perkin-Elmer FTIR spectrometer.

The preparation of pure gaseous PAN samples is hazardous owing to the inherent explosive and toxic nature of the compound and required a dedicated system for gas handling. The PAN gas was extracted from the dodecane solvent using liquid nitrogen freeze-pump-thaw cycles on a high vacuum line. Due to the potential for errors arising from chemical loss rates of PAN to thermolysis and photolysis, samples were transferred to the absorption cell as quickly as possible after isolation from the solvent. Background scans for the evacuated spectrometer and cell were obtained immediately prior to and following each spectral measurement of PAN.

3. Contaminant corrections

A number of spectral signatures due to contaminants were identified in the PAN spectra. Efforts were made to remove these contaminants during the measurements. However these were not entirely successful and therefore residual features were removed in the subsequent analysis. The removal procedure adopted varied according to whether the spectral contamination was in the form of spectral lines or broad absorption bands.

Once the contaminant signatures have been removed, absolute absorption cross-sections can be calculated using the Beer-Lambert law

$$I = I_0 \times 10^{(-n\sigma x)} \quad (1)$$

where n is the target gas number density (molecules m^{-3}), σ is the absorption cross-section (m^2 molecule^{-1}) and x is the absorption cell path length (m). The I/I_0 term represents the transmission spectra recorded in the experiment.

ACPD
4, 5655–5681, 2004

3.1. Line contaminants

Contamination from water vapour, carbon dioxide and nitrogen dioxide were observed in some of the PAN samples used in this experiment. Carbon dioxide (CO_2) along with other dissociated products (Miller et al., 1999) is produced by the breakdown of PAN during storage. Products other than carbon dioxide are not believed to be present in the measured sample as they are expected to remain in solution or to be removed during the freeze-pump-thaw process.

Various methods were employed to reduce sample impurities. Freshly prepared samples gave the best results, with negligible carbon dioxide levels. Long-term storage of prepared samples of over a week led to greater levels of impurity. Opaque black shielding around the apparatus reduced photolysis of PAN, which could produce nitrogen dioxide and N_2O_4. Care was taken to ensure as complete as possible drying with magnesium sulphate during synthesis.

The effect of contaminants on the determination of absorption cross-sections is twofold. Firstly, the contribution to the number density term in Eq. (1) from the contaminants must be removed. Secondly, the measured spectra should be corrected for the presence of contaminant spectral lines. The concentration, and hence number density contribution from line contaminants, was calculated by fitting the contaminant spectral lines using an optimal estimation technique described by Rodgers (2000), which provides a non-linear inverse fitting technique with mathematical error estimation. The spectral ranges used for this fitting method are shown in Table 2. Line parameters for the contaminating gases were obtained from the HITRAN database (Rothman, 1992) and modelled spectra were produced using the Oxford Reference Forward Model (RFM) described by Dudhia (http://www.atm.ox.ac.uk/RFM/). Example fits are shown in Fig. 1 for the retrieval of line contaminant concentrations for carbon dioxide and water vapour as the retrieved temperature and pressure. The residuals obtained demonstrate the excellent performance of this retrieval method. The remaining residual is predominantly instrumental baseline noise.

ACPD
4, 5655–5681, 2004

3.2. Broadband contaminants

An initial ambiguity in the relative intensity of the 1741 cm^{-1} ($\nu_{as}(NO_2)$) PAN band led to an investigation of differences between spectra recorded with different samples. It was concluded that a number of the spectra included subtle signatures of acetone vapour. The acetone spectrum includes a band of broad shape centred also at 1741 cm^{-1}.

Acetone ($CH_3C(O)CH_3$) may be a product of reactions both in the stored sample and in the gas phase and may also be present during synthesis and hence dissolved with PAN in dodecane at this point. No other contaminant spectral features were observed other than those already discussed, with the exception of trace quantities of NO_2 in some samples, which is a product of PAN thermolysis (Bruckmann and Willner, 1983). The only effect on this study was that many recorded spectra in this region had to be discarded, resulting in fourteen spectra retained for analysis. However, the effect may have some significance for the accuracy of previous studies.

4. Results and discussion

Contaminant partial pressures were subtracted from the measured cell pressure before calculation of PAN cross-sections, absorptivities and integrated intensities. Other sources of error were considered before determining the PAN concentration including the contribution of air leaks to the measured pressures and the rate of decrease in PAN concentration as discussed in the previous section.

There remains the possibility of the presence of non-infrared active gas species in the sample that are not introduced by air leaks but through release of such gases dissolved in the dodecane. Such errors would be systematic for all bands in individual recorded spectra but can vary from sample to sample. However, since relative band intensities are derived from linear fits (see later), the resulting error on, for example, integrated band intensities is always to systematically decrease the derived cross-section and to introduce random uncertainty into the line fit used.

4.1. Cross-section calculation

Figure 2 shows PAN cross-sections derived from three spectra with the most accurate removal of contaminants. The resultant PAN cross-sections exhibit an excellent zero baseline reflecting the quality of the instrument and detectors used for this investigation. The band centre positions are in excellent agreement with those reported for PAN in previous studies (Stephens, 1969; Gaffney et al., 1984; Bruckmann and Willner, 1983; Niki et al., 1985; Tsalkani and Toupance, 1989). We use the band assignments for PAN previously reported by Gaffney et al. (1984) and Bruckmann and Willner (1983).

The low noise level of the FTIR cross-section shown in Fig. 2 allows the very weak 590 cm^{-1} (ν_{22}), 720 cm^{-1} (wag(NO_2)) and 1375 cm^{-1} ($\delta_s CH_3$) bands to be observed. However, these bands are not easily analysed here because of detector cut-off and associated noise, signal-to-noise ratio, and the complexity of the band structure respectively. Hence results here are limited to the five main bands and to the weaker 606, 930, 991 and 1055 cm^{-1} bands.

4.2. Infrared absorptivities

Figure 3 shows peak absorbances measured for each of the five principal PAN bands plotted against determined PAN partial pressure. Infrared absorptivities are determined from the slope of the linear regression fits of $A = f(P)$, where A is absorbance and P is pressure. Absorbance is calculated as usual as the negative logarithm to the base 10 of the transmission, defined in Sect. 3. Work by Tsalkani and Toupance (1989), on determining infrared absorptivities for the same five absorption bands over a pressure range of 0.40 to 11.61 hPa showed linearity of Beer's law. This work, although over a smaller pressure range, also confirms this linearity over the pressure range 0.21–2.20 hPa.

The individual error bars plotted in Fig. 3 were derived considering the following for each measurement: Vacuum line leak rate (typically 1–5% uncertainty in total pressure), cell adsorption (derived from cell pressure gradient, 1–3%), PAN decomposition

ACPD
4, 5655–5681, 2004

(0–1% equivalent pressure error), temperature drift (effects calculated cross-section), pressure measurement error (<0.3%), uncertainty in infrared active contaminants (0–10% of measured pressure), instrument background drift and noise (negligible for integrated intensities). For the data points with largest errors, uncertainty in the determination of the contaminant concentration is the dominant factor.

There is very little scatter around the fitted regression lines, although two experimental points are not fitted within the known error budget in the 794 (δ (NO_2)), 1163 (ν (C-O)) and 1302 cm^{-1} (ν_s (NO_2)) bands.

The derived infrared absorptivities for the band centres of the five principal PAN bands are shown in Table 3 with a comparison to previous studies. The first reported absorptivities for four of the weaker PAN bands in the mid infrared are also calculated from the same spectra and are shown in Table 4. There is excellent agreement in Table 3 for the 794, 1163 and 1302 cm^{-1} bands with respect to work by Tsalkani and Toupance (1989) and by Niki et al. (1985). However, a significant difference exists between the datasets for the 1842 cm^{-1} band with a 15% difference with the Tsalkani and Toupance (1989) result and 7% with that reported by Niki et al. (1985). The reason for this difference is unclear. The higher absorptivities reported for the 1741 cm^{-1} PAN band in earlier studies at lower resolutions could be subject to interference from a noted contaminant water vapour absorption line centred at 1739.850 cm^{-1}. This contaminant absorption line would not be resolved from the 1741 cm^{-1} PAN band centre at spectral resolutions below 0.5 cm^{-1} such as those resolutions employed by all but Niki et al. (1985) and in this work. Some water vapour contamination was noted in those studies detailed in Table 3. This interference could contribute positively to the calculated absorptivity in low-resolution studies giving positively biased data for the absorptivity of the 1741 cm^{-1} band.

A detailed comparison could also be performed for integrated intensities. This quantity, in principle, is not subject to resolution effects as the bandwidth considered is suitably large relative to the resolution so long as there is no spectral saturation present.

ACPD
4, 5655–5681, 2004

4.3. Integrated band intensities

Integrated band intensities for the five main bands of PAN were determined by summing the absorbances over the spectral ranges detailed in Table 5. The integrated band area for the 794 cm^{-1} absorption band, which interferes with a smaller band centred at 822 cm^{-1}, is calculated using a vertical truncation at the absorbance minimum between the 794 and 822 cm^{-1} bands.

The results plotted in Fig. 4 show excellent internal consistency given the low partial pressures and limited pressure range of PAN measured. Again, only small scatter around the calculated regression fits is observed although some points remain unfitted within the known error budget. The pressure range was limited in these experiments by the desire to avoid spectral saturation effects that would have occurred due to the long path length of the absorption cell used.

The integrated absorption intensities were determined from the slopes of the least squares linear regression fits and are compared with data from previous studies in Table 6. The errors shown for the work here represent one standard deviation of the total individual error contributions from the calculated mean integrated intensity reported. Integrated intensities for the weaker 606, 930, 991 and 1055 cm^{-1} bands are shown in Table 7.

Our integrated absorption intensity data compare well with those of Tsalkani and Toupance (1989) with a minimum 0.8% difference in the 794 cm^{-1} absorption band and a maximum 10.6% difference in the 1163 cm^{-1} band. Comparing our data with that originally reported by Gaffney et al. (1984), however, we see differences ranging from 2.5% for the 794 cm^{-1} band and 50.5% for the 1741 cm^{-1} band (see later). Large differences were also reported by Tsalkani and Toupance (1989) in their comparison with the Gaffney et al. (1984) data. The results from this work are therefore in better agreement with those of Tsalkani and Toupance (1989). Firstly, this work has found a 4.8% lower intensity for the 1741 cm^{-1} band. Secondly this work calculates the 1163 cm^{-1}(ν (C-O)) band intensity to be 10.6% higher than the data of Tsalkani and

ACPD
4, 5655–5681, 2004

Toupance (1989).

A constant relative difference between all bands would indicate a systematic error due to incorrect pressure measurements for example as noted by Tsalkani and Toupance (1989), who also noted that there may be impurities in the PAN sample contributing to some bands. Tsalkani and Toupance (1989) assert that their PAN samples were >98% pure as determined by gas chromatography and state that the only contaminants identified were carbon dioxide and water vapour. These contaminants are clearly seen in the Tsalkani and Toupance (1989) spectrum with water lines visible in the 1600–1650 cm^{-1} spectral region, even with a relatively low resolution of 1 cm^{-1}.

An informative way to analyse the effects of any contaminants that may be contaminating a band is to consider the relative intensity of each band with respect to a band which shows the best internal consistency and is known to be free from any contaminants that may be thought to be present. The 794 cm^{-1} absorption band is chosen for this purpose here since it shows the best agreement with previous work; Tsalkani and Toupance (1989) employed the 1842 cm^{-1} band for which some absolute intensity disagreements may still exist. The relative intensities for this work are calculated for each independent measurement and averaged to give the results shown in Table 8. In the table, we show the results of Tsalkani and Toupance (1989) together with their re-evaluation of the Gaffney et al. (1984) data; the relative intensities originally reported by Gaffney et al. (1984) seem to be incorrect.

The largest differences in the relative ratios are seen for the 1741 cm^{-1} PAN band. It is possible on the basis of this result that measurement of the 1741 cm^{-1} absorption band in earlier studies may have been effected by the same contamination by acetone seen in our discarded spectra.

5. Conclusions

Cross-sections of PAN vapour at spectral resolutions of 0.03 cm^{-1} and 0.25 cm^{-1} have been determined in the mid-infrared range of 550–2200 cm^{-1} at 295 K.

ACPD
4, 5655–5681, 2004

Integrated band intensities for the five main bands of PAN are seen to be generally in good agreement with earlier work by Tsalkani and Toupance (1989) supporting these results rather than those of Gaffney et al. (1984). The integrated intensity of the 1163 cm^{-1} PAN band is noted to show the greatest inconsistency between the datasets. We now believe that the PAN band intensities at room temperature are now accurate to within 10%.

The nature of a difference in the integrated intensity reported for the 1741 cm^{-1} band in the datasets studied remains unresolved although it is proposed here that contamination by acetone in this band may be a source of error in previous measurements. We believe similar contamination may have resulted in an overestimation of the reported integrated intensity for the 1741 cm^{-1} band in previously reported data.

In addition, probable contamination from water vapour and carbon dioxide concentrations were not removed in previous calculations of PAN absorption cross-sections. Spectral fitting and partial pressure correction of contaminants in the Gaffney et al. (1984) and Tsalkani and Toupance (1989) datasets are imperative if these data are to be used in quantitative applications. Without access to previous datasets it is difficult to confirm the effects of contamination on their results.

Finally, new integrated band intensities and band centre absorptivities have been reported in this work for the weak PAN absorption bands centred at 606, 930, 990, and 1055 cm^{-1}.

Acknowledgements. The authors wish to thank the Natural Environment Research Council (NERC) for supporting G. Allen thorough grant ref: NER/T/S/2000/01087, and for access to the Molecular Spectroscopy Facility at the Rutherford Appleton Laboratory (RAL). R. G. Williams is thanked for providing technical support at the Rutherford Appleton Laboratory.

References

Bruckmann, P. W. and Willner, H.: Infrared spectroscopic study of peroxyacetyl nitrate (PAN) and its decomposition products, Envir. Sci. Tech., 17, 352–357, 1983.

Emmons, L. K., Carroll, M. A., Hauglustaine, D. A., Brasseur, G. P., Atherton, C., Penner, J., Sillman, S., Levy II, H., Rohrer, F., Wauben W. M. F., van Velthoven, P. F. J., Wang Y., Jacob, D. J., Bakwin, P., Dickerson, R., Doddridge, B., Gerbig, C., Honrath, R., Hubler, G., Jaffe, D., Kondo, Y., Munger, J. W., Torres, A., and Volz-Thomas, A.: Climatologies of NO_x and NO_y: a comparison of data and models, Atmos. Envir., 31, 1851–1903, 1997.

Fischer, H. and Oelhaf, H.: Remote sensing of vertical profiles of atmospheric trace constituents with MIPAS limb-emission spectrometers, Appl. Optics, 35, 2787–2796, 1996.

Gaffney, J. S., Fajer, R., and Senum, G. I.: An improved procedure for high purity gaseous peroxyacetyl nitrate production: Use of heavy lipid solvents, Atmos. Envir., 18, 215–218, 1984.

Kirchener, F., Mayer-Figge, A., Zabel, F., and Becker, K. H.: Thermal stability of peroxynitrates, Int. J. Ch. K., 31, 127–144, 1999.

Louet, J.: The Envisat mission and system, ESA Bulletin – European Space Agency, (106), 11–25, 2001.

Miller, C. E., Lynton, J. I., Keevil, D. M., and Francisco, J. S.: Dissociation pathways of Peroxyacetyl Nitrate (PAN), J. Phys. Chem. A, 103, 11 451–11 459, 1999.

Nett, H., Frerick, J., Paulsen, T., Levrini, G.: The atmospheric instruments and their applications: GOMOS, MIPAS and SCIAMACHY, ESA Bulletin – European Space Agency, (106), 77–87, 2001.

Nielsen, T.: A convenient method for preparation of pure standards of peroxyacetyl nitrate for atmospheric analyses, Atmos. Envir., 16, 2447–2450, 1982.

Niki, H., Maker ,P. D., Savage, C. M., and Breitenbach, L. P.: An FTIR spectroscopic study of the reactions Br + $CH_3CHO \rightarrow$ HBR + CH_3CO and $CH_3C(O)OO + NO_2 \leftrightarrow CH_3C(O)OONO_2$(PAN), Int. J. Ch. K., 17, 525–534, 1985.

Norton, R. H. and Beer, R.: New apodising functions for Fourier spectrometry, J. Opt. Soc. A., 66, 259–264, 1976.

Norton, R. H. and Beer, R.: New apodising functions for Fourier spectrometry – Erratum. J. Opt. Soc. A., 67, 419, 1977.

Olszyna, K. J., Bailey, E. M., Simonaitis, R., and Meagher, J. F.: O_3 and NO_y relationships at a rural site, J. Geophys. Res-A., 99, 14 557–14 563, 1994.

Rothman, L. S.: The HITRAN database, J. Quan. Spect., 48, 469–507, 1992.

Rodgers, C. D.: Inverse methods for atmospheric sounding: Theory and practice (Series on atmospheric, oceanic and planetary physics), World Scientific Publishing, 2000.

ACPD

4, 5655–5681, 2004

Singh, H. B.: Reactive nitrogen in the troposphere - chemistry and transport of NO_x and PAN, Envir. Sci. Technol., 21, 320–327, 1987.

Talukdar, R. K., Burkholder, J. B., Schmoltner, A., Roberts, J. M., Wilson, R. R., and Ravishankara, A. R.: Investigation of the loss processes for peroxyacetyl nitrate in the atmosphere: UV photolysis and reaction with OH, J. Geophys. Res-A., 100, 14 163–14 173, 1995.

Tsalkani, N. and Toupance, G.: Infrared absorptivities and integrated band intensities for gaseous peroxyacetyl nitrate (PAN), Atmos. Env., 23, 1849–1854, 1989.

Table 1. Configuration of the Bruker IFS120 HR spectrometer for PAN sample measurements. Norton-Beer strong apodisation function based on that described by Norton and Beer (1976) and Norton and Beer (1977).

Spectrometer Configuration	
Resolution (nominal)	0.03/0.25 cm^{-1}
Beamsplitter	Ge/potassium bromide (KBr)
FTIR input aperture	1.0 mm
Detector	Broadband liquid nitrogen-cooled mercury cadmium telluride (MCT-D390)
Source	Globar
Apodisation function	Norton-Beer strong
Gas cell	26.1 cm glass (evacuable)
Cell windows	Wedged KBr

ACPD
4, 5655–5681, 2004

Table 2. Spectral fitting ranges for retrieval of contaminant gas concentrations for carbon dioxide and water vapour.

Species	Window 1 range/cm^{-1}	Window 2 range/cm^{-1}	Window 3 range/cm^{-1}
CO_2	643–697	2255–2385	3560–3750
H_2O	1465–1575	1480–1625	

ACPD
4, 5655–5681, 2004

Table 3. Infrared absorptivities for gaseous PAN (10^{-1} ppm^{-1} m^{-1}, log to base 10 to 3 s.f., values refer to 1013.25 hPa) for five principal PAN bands. Errors quoted represent one standard deviation of individual error contributions for each sample.

Band centre position/cm^{-1}					Resolution	
794	1163	1302	1741	1842	/cm^{-1}	Ref.
10.1	14.3	11.2	23.6	10.0	>5.00	Stephens (1964)
13.4	15.8	13.6	32.6	12.4	1.20	Bruckmann and Willner (1983)
11.5±0.6	14.5±0.7	11.3±0.6	31.0±1.6	10.2±0.5	0.06	Niki et al. (1985)
12.2±0.2	15.7±0.3	11.9±0.2	31.4±0.8	10.9±0.2	1.00	Tsalkani and Toupance (1989)
11.4±0.4	14.6±0.5	11.4±0.4	30.2±1.5	9.5±0.6	0.03/0.25	This work

ACPD
4, 5655–5681, 2004

Table 4. Infrared absorptivities for gaseous PAN (10^{-1} ppm^{-1} m^{-1}, log to base 10 to 3 sig. fig. Values refer to 1013.25 hPa) for the weaker 606, 930, 991 and 1055 cm^{-1} absorption bands. Errors quoted represent one standard deviation of individual error contributions for each sample.

Band centre position/cm^{-1}			
606	930	991	1055
1.55±0.06	1.46±0.06	1.03±0.04	0.62±0.03

ACPD
4, 5655–5681, 2004

Table 5. Spectral ranges used to calculate integrated band areas for the nine PAN absorption bands studied.

Band centre position/cm^{-1}	Integration range/cm^{-1}
606	585.0–652.0
794	767.4–810.2
930	900.1–956.0
991	967.5–1008.1
1055	1035.0–1075.1
1163	1115.3–1210.2
1302	1260.7–1333.0
1740	1685.8–1780.0
1841	1802.0–1875.3

ACPD
4, 5655–5681, 2004

Table 6. Infrared integrated intensities ($atm^{-1}\,cm^{-2}$ to 3.s.f) of the 794, 1163, 1302, 1741 and 1842 cm^{-1} PAN bands with comparison to work by Gaffney et al, 1984 and Tsalkani and Toupance, 1989. (Units refer to 1 atm at ambient temperature 291 K unless otherwise stated).

Band centre position/cm^{-1}					
794	1163	1302	1741	1842	Reference
247±6	477±9	405±20	808±34	322±9	Gaffney et al. (1984) original data
239±4	322±7	270±2	563±10	262±4	Tsalkani and Toupance (1989)
241±3	356±4	281±3	537±5	260±3	This work (295 K)

Table 7. Infrared integrated intensities (atm^{-1} cm^{-2} to 3.s.f) of the 606, 930, 991 and 1055 cm^{-1} PAN bands: (Units refer to 1 atm at 295 K).

Band centre position/cm^{-1}			
606	930	991	1055
34.2±0.7	32.2±0.6	20.1±0.4	16.0±0.4

ACPD
4, 5655–5681, 2004

Table 8. Relative integrated absorption intensities normalised to the 794 cm^{-1} band intensity. The quoted data from Gaffney et al. (1984), are based on a re-evaluation of the Gaffney et al. (1984) results performed by Tsalkani and Toupance (1989).

Band centre position/cm^{-1}	Re-evaluation of data reported by Gaffney et al. (1984)	Tsalkani and Toupance (1989)	This work
794	1.00	1.00	1.00
1163	1.33	1.39	1.47
1302	1.13	1.13	1.16
1741	2.11	2.36	2.23
1842	1.10	1.10	1.08

ACPD
4, 5655–5681, 2004

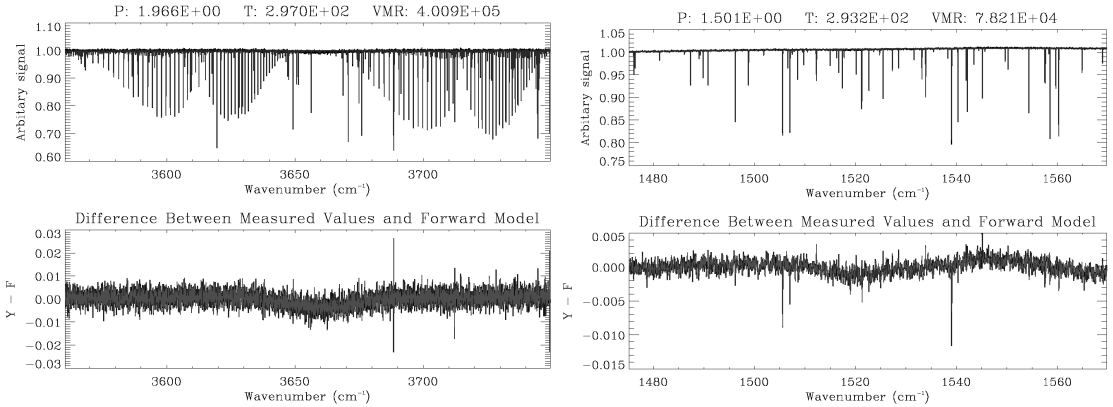

Fig. 1. Spectral fit and residual for a sample showing contamination with water vapour and carbon dioxide. The sample concerned was recorded at a resolution of 0.03 cm^{-1} at 295 K. Retrieved pressure (mb), temperature (K) and concentration (ppmv) of contaminant are shown for each contaminant. The plots show **(a)** Recorded transmission spectrum over 1470–1570 cm^{-1}, **(b)** Residual of fit to transmission spectrum for H_2O, **(c)** Recorded transmission spectrum over 3560–3750 cm^{-1}, **(d)** Residual of fit to transmission spectrum for CO_2.

ACPD
4, 5655–5681, 2004

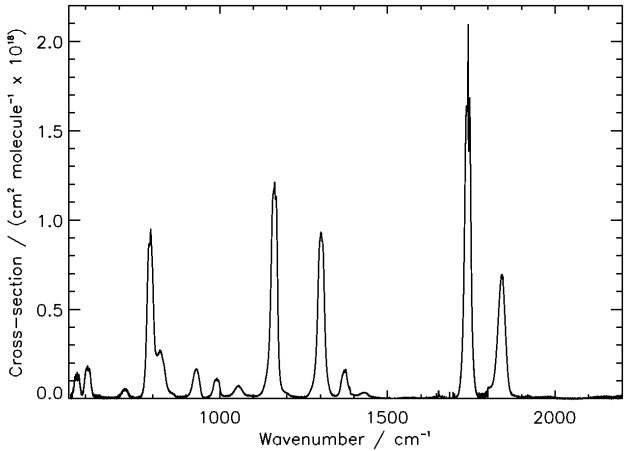

Fig. 2. Derived PAN absorption cross section, Temperature=295 K±1 K, unapodised resolution=0.03 cm^{-1}.

ACPD
4, 5655–5681, 2004

High resolution mid-infrared cross-sections for PAN

G. Allen et al.

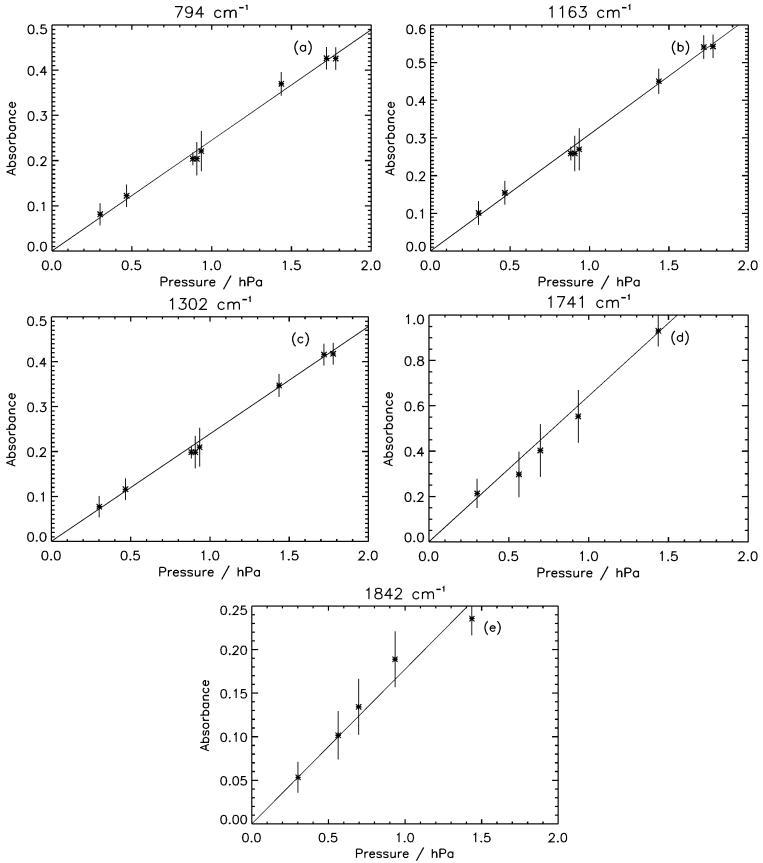

Fig. 3. Infrared absorptivities taken at the quoted band centre as a function of PAN pressure for **(a)** 794 cm^{-1}, 11 samples, **(b)** 1163 cm^{-1}, 11 samples, **(c)** 1302 cm^{-1}, 11 samples, **(d)** 1741 cm^{-1}, 5 samples and **(e)** 1842 cm^{-1}, 5 samples. Errors shown are for the sum of all known error contributions for each sample.

ACPD
4, 5655–5681, 2004

High resolution mid-infrared cross-sections for PAN

G. Allen et al.

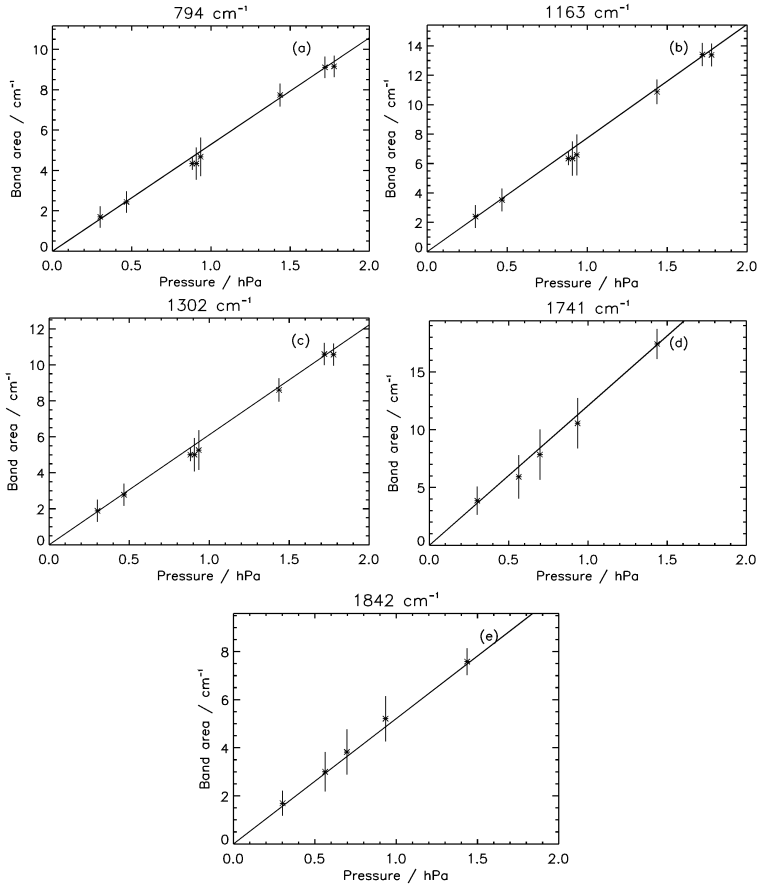

Fig. 4. Integrated PAN band areas calculated as a function of PAN pressure for **(a)** 794 cm^{-1}, 11 samples, **(b)** 1163 cm^{-1}, 11 samples, **(c)** 1302 cm^{-1}, 11 samples, **(d)** 1741 cm^{-1}, 5 samples and **(e)** 1842 cm^{-1}, 5 samples. Errors shown are for the sum of all known error contributions for each sample.

ACPD
4, 5655–5681, 2004

High resolution mid-infrared cross-sections for PAN

G. Allen et al.